AEM
Journals.ASM.org

Trimethylamine and Organic Matter Additions Reverse Substrate Limitation Effects on the $\delta^{13}C$ Values of Methane Produced in Hypersaline Microbial Mats

Cheryl A. Kelley,[a] Brooke E. Nicholson,[a]* Claire S. Beaudoin,[a] Angela M. Detweiler,[b] Brad M. Bebout[b]

Department of Geological Sciences, University of Missouri, Columbia, Missouri, USA[a]; Exobiology Branch, NASA Ames Research Center, Moffett Field, California, USA[b]

Methane production has been observed in a number of hypersaline environments, and it is generally thought that this methane is produced through the use of noncompetitive substrates, such as the methylamines, dimethylsulfide and methanol. Stable isotope measurements of the produced methane have also suggested that the methanogens are operating under conditions of substrate limitation. Here, substrate limitation in gypsum-hosted endoevaporite and soft-mat hypersaline environments was investigated by the addition of trimethylamine, a noncompetitive substrate for methanogenesis, and dried microbial mat, a source of natural organic matter. The $\delta^{13}C$ values of the methane produced after amendments were compared to those in unamended control vials. At all hypersaline sites investigated, the $\delta^{13}C$ values of the methane produced in the amended vials were statistically lower (by 10 to 71‰) than the unamended controls, supporting the hypothesis of substrate limitation at these sites. When substrates were added to the incubation vials, the methanogens within the vials fractionated carbon isotopes to a greater degree, resulting in the production of more ^{13}C-depleted methane. Trimethylamine-amended samples produced lower methane $\delta^{13}C$ values than the mat-amended samples. This difference in the $\delta^{13}C$ values between the two types of amendments could be due to differences in isotope fractionation associated with the dominant methane production pathway (or substrate used) within the vials, with trimethylamine being the main substrate used in the trimethylamine-amended vials. It is hypothesized that increased natural organic matter in the mat-amended vials would increase fermentation rates, leading to higher H_2 concentrations and increased CO_2/H_2 methanogenesis.

Both soft and gypsum-hosted endoevaporite microbial mats can be found in hypersaline environments, with soft mats dominating at lower salinities and endoevaporites at higher salinities (see, for example, reference 1). Organisms living in these hypersaline microbial mat environments need to be able to regulate osmotic pressures within the cell, and most do it using organic solutes (2), with glycine betaine found to be one of the leading organic osmotic solutes (3). Glycine betaine degrades to trimethylamine (TMA) (4, 5), which is a substrate that can be used by methanogens within the mat. Although the two main substrates used by methanogens are CO_2/H_2 and acetate, high sulfate concentrations in hypersaline environments and the well-known competition for H_2 and acetate between sulfate reducers and methanogens (6) allow the noncompetitive substrates, such as TMA, to be the dominant substrates used by methanogens in hypersaline environments (7–9). Other noncompetitive substrates include methanol, which is an end product of pectin degradation (10) and can be produced by phytoplankton (11), and dimethylsulfide, which is derived from dimethylsulfionopropionate, an osmolyte found in higher plants and algae (12).

Sources of methane, whether biogenic (produced by methanogenic *Archaea* using the substrates above) or thermogenic (produced from the breakdown of organic matter under high temperatures and pressures), can be identified by their stable isotopic composition. Biogenic methane results in $\delta^{13}C$ values below ~−50‰ and thermogenic methane in $\delta^{13}C$ values above ~−50‰ (13). Oxidation of the produced methane can affect this delineation, since oxidation results in the remaining methane becoming enriched in the heavier isotopes of both C and H (14). In recent work, Tazaz et al. (1) reported biogenic methane produced at hypersaline sites, with no evidence of oxidation occurring, having $\delta^{13}C$ values greater than −50‰, with some as high as −35‰, which fall considerably outside the range generally considered biogenic. The most ^{13}C-enriched biogenic methane was produced from the gypsum-hosted endoevaporite mats, as opposed to soft microbial mats, which were also found at their sites (1). These anomalously high, ^{13}C-enriched $\delta^{13}C$ values for biogenic methane have been hypothesized to be the result of substrate limitation occurring within the gypsum crusts (9).

In the present study, the generality of this hypothesis was tested at additional hypersaline sites in the Atacama Desert of Chile, as well as sites in Guerrero Negro, Mexico (also examined in references 1 and 9). Methane production rates and isotopic composition, as well as particulate organic carbon (POC) content and $\delta^{13}C$ values, were measured at these sites, which contain both soft microbial mats and endoevaporite mats. Since TMA is the main substrate used by methanogens at hypersaline sites (see, for example, references 7, 8, and 9), high concentrations of TMA were added to incubation vials to alleviate substrate limitation, and the stable isotopic composition of the methane produced was determined. In addition, dried, autoclaved soft microbial mat material from a hypersaline environment, a source of natural organic matter, was

Received 11 August 2014 **Accepted** 12 September 2014
Published ahead of print 19 September 2014
Editor: C. R. Lovell
Address correspondence to Cheryl A. Kelley, kelleyc@missouri.edu.
* Present address: Brooke E. Nicholson, URS Corporation, Omaha, Nebraska, USA.

doi:10.1128/AEM.02641-14

also added to incubation vials. The resultant $\delta^{13}C$ value of the methane produced was measured to ascertain the effects of increased organic matter content on methane production. We found that both TMA-amended and microbial mat-amended samples produced methane with $\delta^{13}C$ values much lower than that of the unamended controls. These results indicate that the methanogens are operating under substrate limitation *in situ*, which can be alleviated by the addition of either methanogenic substrates or precursors of those substrates in the form of natural organic matter.

MATERIALS AND METHODS

Two main field areas were investigated: the salt ponds of the Exportadora de Sal, S.A. de C.V., salt company located in Guerrero Negro, Baja California Sur, Mexico, and the Atacama Desert, northern Chile (Fig. 1). The methane biogeochemistry at the Guerrero Negro salterns, the largest solar salt works in the world, has been studied for a number of years (1, 9, 15–17). At the Guerrero Negro salt works, samples were collected in March 2012 and November 2012 from Areas 1 and 9 (Table 1), with salinities of ~60 (Area 1) and ~160 (Area 9) parts per thousand (ppt). The Area 1 samples consisted of soft, thick microbial mats, while Area 9 contained gypsum crusts containing colorful endoevaporitic microbial communities.

The other sampling sites were located within the Atacama Desert in Chile, the oldest and driest desert on Earth, receiving <1 mm of rainfall annually (18). The Atacama sites were sampled in May 2012 and 2013 (Table 1). In May 2012, samples from three different gypsum crusts (LL1 to LL3) were obtained from the largest of many hypersaline ponds at Salar de Llamara. The salinity of the overlying water was ~130 ppt. In addition, a small, cool pool, ET2, was sampled at the El Tatio volcanic geyser field, the largest geothermal area in the Southern Hemisphere. The salinity at this site was ~13 ppt (about 1/3 that of seawater), and the sample consisted of organic-rich muddy sediments (approximately the upper 25 cm was collected). Although this site is not strictly hypersaline (i.e., salinity greater than seawater), it provided a low-salinity end-member. In May 2013, the same sites at Salar de Llamara and El Tatio were again sampled. Another small pool (~55 ppt) containing a soft microbial mat at the Salar de Llamara was also sampled (LL8). Furthermore, samples from two lagoons, Laguna Cejar and Laguna Chaxa, in the Salar de Atacama were obtained. Three sites at Laguna Cejar, of which the first two (Cejar1 and Cejar2) were soft microbial mats, were sampled. Salinities here were about 50 ppt. Gypsum crust was sampled at Cejar3, which was located near a deep central pool (salinity of ~77 ppt). The single sample obtained at Laguna Chaxa (Chaxa1) was composed of a thin, soft microbial mat overlying organic-rich mud, with a salinity of ~100 ppt.

A few other sites, including Areas 10 and 11 at Guerrero Negro, and LL4, a small pond at Salar de Llamara, were also sampled. Little, if any, methane was produced at any of these sites (production rates of ≤0.1 nmol g^{-1} day^{-1}), so these sites will not be discussed further here.

From each site, samples of soft mat/mud or gypsum-hosted endoevaporite mat and overlying pond water were collected. Temperature was obtained at the depths where samples were collected. The salinity of site water was measured in the field or shortly thereafter using a hand-held refractometer.

In order to determine methane production rates and $\delta^{13}C$ values from the sites, incubations were prepared in 38-ml serum vials using slurries containing approximately 10 to 20 g (ranging from 6 to 25 g) of homogenized soft mat/mud or crust and 10 ml of site water. Prior to use in incubations, site water was bubbled with N_2 gas for at least 10 min to remove dissolved O_2. Unamended control slurries contained only soft mat/mud or crust and 10 ml of site water, while either TMA or dried microbial mat material was added to additional incubation vials. TMA, with a $\delta^{13}C$ value of −40‰, was added to incubation vials to a final concentration of 1,000 μM in order to determine the $\delta^{13}C$ values of methane produced when the amount of substrate is not limiting. At a few sites, dried microbial mat material was added (1 g/vial) to slurries to investigate the effects of higher concentrations of organic matter. The mat was obtained from Area 4 of the Exportadora de Sal salt works in Guerrero Negro. The soft microbial mats of Guerrero Negro have been studied over many years (19–25). For the purposes of the present study, the microbial mat was autoclaved to kill any microorganisms and dried to remove moisture; this treatment (autoclaving/drying) would have also removed any volatile compounds, such as TMA. This autoclaved, dried microbial mat had a bulk POC $\delta^{13}C$ value of −11‰ and a POC concentration of 12%. Once site water and any amendments were added, all incubation vials were stoppered and the headspaces of all vials were flushed with N_2 gas for 5 min to remove any O_2 gas in the headspace. Vials were inverted and incubated undisturbed at room temperature in the dark. Before measurements for methane concentrations, the vials were shaken for at least 2 min to drive dissolved methane up into the headspace.

Methane production rates were determined by measuring methane concentration in the headspace of incubation vials at known time intervals. Concentrations were measured with a gas chromatograph equipped with a flame ionization detector and Porapak Q column. The frequency of sampling was adjusted based on how quickly methane concentrations increased in the headspace. Upon reaching concentrations greater than ~1,000 ppm, an adequate methane concentration for obtaining $\delta^{13}C$ values with our instrumentation, samples were frozen (still inverted) to stop biological activity. Incubations lasted anywhere from about 2 days to about 2 months.

A linear regression fitted to a plot of methane concentration over time was used to calculate methane production rates for each incubation vial. Methane production in some samples began to exhibit exponential increases in concentration over time. In these cases, only the initial linear portions of the curves (portions with r^2 values of ~0.9 or greater) were used to determine production rates. Methane production rates were normalized to the total amount of sample incubated and reported in nmol g^{-1} day^{-1}.

At the end of the incubation, the headspace gas was analyzed for methane $\delta^{13}C$ values using a gas chromatograph with a 60-m PoroPLOT capillary column in line with a ThermoQuest Finnigan Delta Plus XL isotope ratio mass spectrometer (IRMS). Samples were thawed and, depending on the headspace methane concentrations, between 25 and 600 μl of gas was injected into the gas chromatograph. For samples that had methane concentrations less than ~2,000 ppm, a cryofocusing method (26) was used. This cryofocusing method allows for injections of larger volumes of gas for $\delta^{13}C$ determinations at lower methane concentrations.

POC content and $\delta^{13}C$ values were determined from samples of the soft mat/mud or crust used in the incubation slurries. These samples were collected in triplicate in precombusted (450°C for 6 h) 20-ml glass vials. Each POC sample was refrigerated in the field following collection. Upon return to the laboratory, these samples were dried at approximately 65°C and homogenized using mortar and pestle. Inorganic carbon was removed by treatment with hydrochloric acid (HCl). In accordance with the method of Hedges and Stern (27), each sample was weighed and treated with 2 ml of 1 N HCl daily until all visual signs of chemical reaction between acid and carbonate had ceased. Decarbonation took up to 2 weeks for some samples. After removal of the inorganic carbon, samples were dried again and loaded into tin capsules for elemental and isotopic composition analyses on an elemental analyzer connected through a ConFlo III to the IRMS. POC concentration values were corrected for the amount of salts formed from the addition of acid during the removal of inorganic carbon.

Error estimates for methane production rates, isotopic composition of methane and POC, and POC concentrations are reported as the standard deviations of triplicate samples, except in rare occurrences when one of the triplicate samples was lost due to instrument malfunction or human error. In those cases, half of the range between the two values is reported as the error.

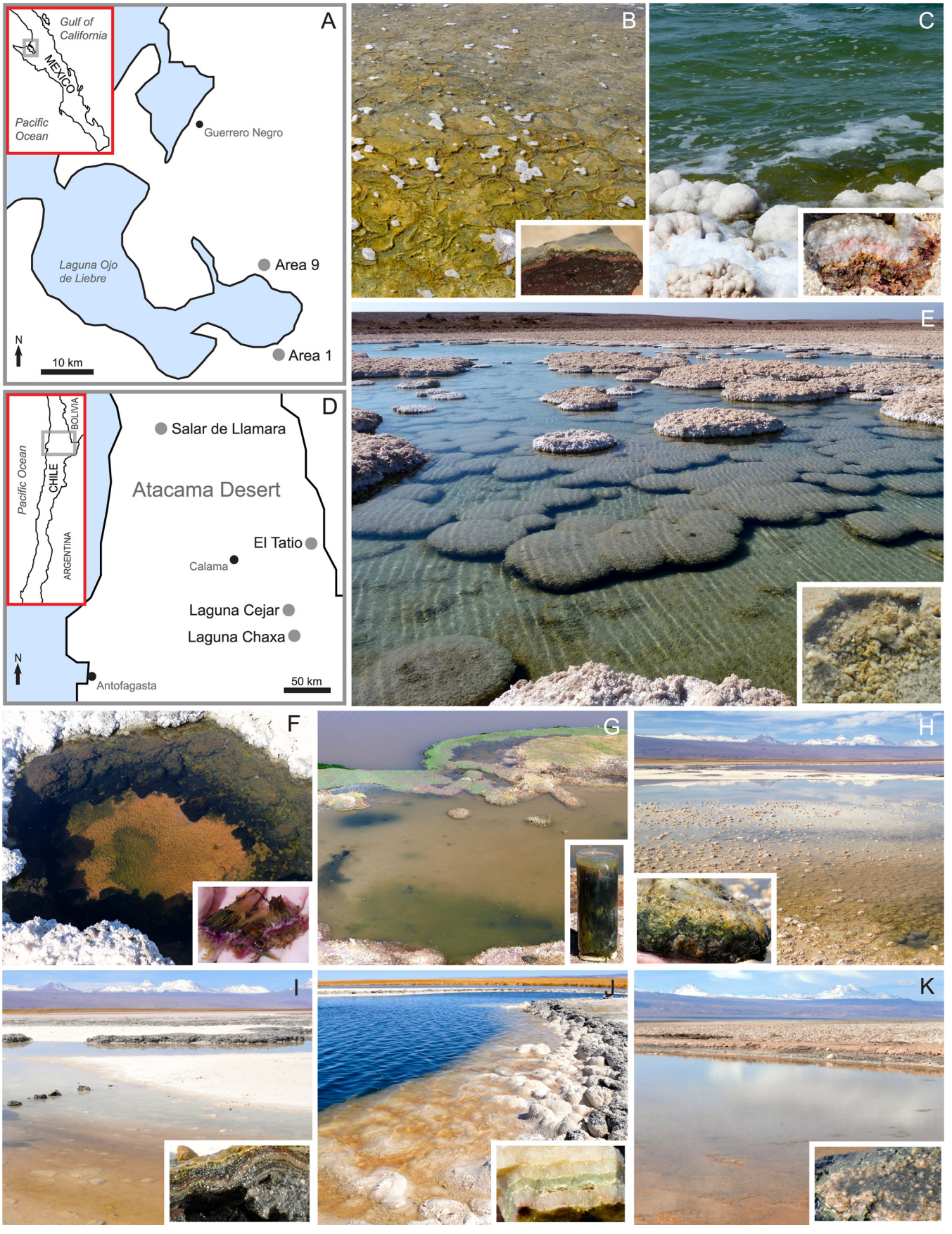
A
Gulf of California
MEXICO
Pacific Ocean
Guerrero Negro
Laguna Ojo de Liebre
Area 9
Area 1
N
10 km
B
C
D
Pacific Ocean
CHILE
BOLIVIA
ARGENTINA
Salar de Llamara
Atacama Desert
El Tatio
Calama
Laguna Cejar
Laguna Chaxa
Antofagasta
N
50 km
E
F
G
H
I
J
K

TABLE 1 Methane production rates and stable isotopic composition for unamended controls, TMA-amended, and mat-amended incubation vials, as well as POC concentration and isotopic composition[a]

Site[b]	Date	Salinity (ppt)	Temp (°C)	Methane production rate (nmol g^{-1} day^{-1})			Methane $\delta^{13}C$ value (‰)			POC	
				Control	TMA	Mat	Control	TMA	Mat	Concn (%)	$\delta^{13}C$ (‰)
Soft-microbial-mat/mud sites											
Area 1	Mar 2012	62	20	5.4 (0.7)	ND[c]	ND	−56.5 (1.7)	ND	ND	17.3 (3.0)	−10.8 (0.5)
Area 1	Nov 2012	60	28	22.5 (3.8)	781 (127)	ND	−46.7 (1.3)	−68.1 (4.3)	ND	10.1 (0.5)	−9.7 (0.2)
ET2	May 2012	13	14	6.0 (2.9)	58.4 (4.2)	112 (2.7)	−75.0 (4.1)	−78.2 (2.1)	−58.8 (0.7)	3.2 (0.04)	−17.7 (0.3)
ET2	May 2013	10	3	289 (5.1)	361 (17.5)	1,910 (158)	−79.0 (0.3)	−79.7 (0.1)	−64.9 (2.0)	4.2 (0.1)	−14.5 (0.1)
LL8	May 2013	55	26	1.3 (0.7)	1.9 (0.2)	ND	−82.6 (0.3)	−93.1 (1.3)	ND	2.3 (0.4)	−10.8 (0.0)
Cejar1	May 2013	45	20	24.0 (19.3)	114 (14.5)	ND	−33.1 (5.0)	−81.7 (0.5)	ND	6.0 (1.3)	−9.7 (0.5)
Cejar2	May 2013	54	22	7.8 (0.9)	39.5(15.9)	ND	−37.8 (1.0)	−82.6 (1.5)	ND	1.8 (0.3)	−11.0 (0.2)
Chaxa1	May 2013	102	20	30.4 (4.5)	193 (7.2)	ND	−30.9 (0.8)	−76.7 (0.4)	ND	3.2 (0.4)	−5.5 (0.2)
Gypsum-hosted endoevaporite mat sites											
Area 9	Mar 2012	160	21	32.4 (4.3)	127 (17.1)	6.5 (1.9)	−28.0 (0.2)	−67.2 (6.6)	−66.0 (1.0)	0.4 (0.1)	−14.6 (0.2)
Area 9	Nov 2012	158	23	21.5 (5.5)	28.0 (8.5)	4.7 (0.2)	−52.7 (4.7)	−79.2 (1.4)	−64.8 (0.6)	0.2 (0.0)	−14.7 (0.2)
LL1	May 2012	130	26	0.4 (0.1)	ND	ND	−37.0 (1.9)	ND	ND	1.1 (0.3)	−10.0 (0.1)
LL2	May 2012	138	25	1.3 (0.4)	5.4 (2.6)	83.3 (28.8)	−31.1 (0.6)	−91.8 (2.6)	−41.7 (12.1)	0.2 (0.02)	−12.0 (0.3)
LL2	May 2013	128	22	1.1 (0.4)	3.6 (0.4)	ND	−20.2 (2.7)	−90.8 (1.0)	ND	0.3 (0.03)	−12.1 (0.2)
LL3	May 2012	131	27	6.8 (1.4)	ND	ND	−32.7 (1.0)	ND	ND	0.5 (0.2)	−10.6 (0.4)
LL3	May 2013	132	23	4.0 (2.5)	4.5 (1.7)	7.3 (3.9)	−43.9 (13.1)	−88.1 (1.6)	−64.0 (1.4)	0.2 (0.04)	−12.2 (0.1)
Cejar3	May 2013	77	13	1.0 (0.1)	1.3 (0.1)	0.7 (0.2)	−35.0 (4.0)	−86.1 (1.2)	−67.0 (2.1)	0.1 (0.01)	−13.0 (0.2)

[a] Error estimates are in parentheses.
[b] That is, sites with methane production rates >0.1 nmol g^{-1} day^{-1} for unamended controls.
[c] ND, not determined.

RESULTS

Methane production rates from unamended control incubations varied across sample sites, with no apparent relationship between production rates and salinity (Fig. 2A). As noted above, a few sites produced little to no methane. Of those that had measurable rates, methane production ranged from 0.4 to 289 nmol g^{-1} day^{-1} (Table 1). The methane $\delta^{13}C$ values also exhibited a very large range (−83 to −20‰) (Table 1), with the higher-salinity, gypsum-hosted sites producing the higher, more ^{13}C-enriched methane $\delta^{13}C$ values (Fig. 2B). The methane $\delta^{13}C$ values at these gypsum sites were significantly more ^{13}C-enriched than sites containing soft mat/mud (Student *t* test, $P < 0.02$).

POC concentrations ranged from 0.1 to 17.3%, with concentrations generally decreasing with increasing salinity (Fig. 2C). The percent POC (%POC) at gypsum-hosted sites was significantly less than the %POC at soft-mat/mud sites (Student *t* test, $P < 0.02$). The POC $\delta^{13}C$ values ranged from −17.7 to −9.7‰ (Table 1), with no relationship to salinity. The $\delta^{13}C$ values of POC at gypsum-hosted sites were not significantly different from soft-mat/mud sites (Student *t* test, $P > 0.4$).

When 1,000 μM TMA was added to incubation vials, methane production was increased over the unamended controls, resulting in production rates ranging from 1.3 to 781 nmol g^{-1} day^{-1} (Table 1). If all of the methane that was produced came from the added TMA, then between 4 and 61% of the TMA was used, with a median value of 9%. The isotopic composition of the methane that was produced ranged from −93 to −67‰ (Table 1; Fig. 3), with no difference between the lower-salinity, soft-mat/mud sites and the higher-salinity, gypsum-hosted sites (Student *t* test, $P > 0.7$). The methane $\delta^{13}C$ values, however, were significantly ^{13}C depleted compared to the unamended controls (paired Student *t* test, $P < 0.01$).

Dried microbial mat material was added (1 g/vial) to samples from five sites (ET2, LL2, LL3, Cejar3, and Area 9), with ET2 and Area 9 being sampled during two different sampling events. This amount of dried mat material increased organic carbon content in vials at all sites by 1.3- to 7-fold. At the four Atacama sites, methane production rates either increased or were not different than the unamended controls, while at Area 9, rates were decreased by the mat addition. Overall methane production rates of mat-

FIG 1 (A) Location of sampling sites at the Exportadora de Sal, S.A. de C.V., salt company near the city of Guerrero Negro in Baja California Sur, Mexico. Soft microbial mats were sampled in Area 1 (B), and gypsum-hosted endoevaporite mats were sampled in Area 9 (C). (D) Sampling sites in the Atacama Desert, northern Chile. Endoevaporitic gypsum crusts (LL1, LL2, and LL3) were collected from the main hypersaline pond (E), whereas LL8, a soft mat, was sampled from a smaller pond (F) at Salar de Llamara. (G) Muddy sediments, ET2, were collected from a cool pond at the El Tatio geyser field. Within the Salar de Atacama, soft mats, Cejar1 (H) and Cejar2 (I), and endoevaporite mats, Cejar3 (J), were sampled at Laguna Cejar, and a soft mat overlying mud, Chaxa1, was sampled at Laguna Chaxa (K). Insets of representative soft mats/mud and gypsum-hosted endoevaporite mats at the sites are also included. (The maps in panel A are traced from images from the CIA World Factbook [https://www.cia.gov/library/publications/the-world-factbook/geos/mx.html] and NASA Earth Observatory [http://earthobservatory.nasa.gov/IOTD/view.php?id=77499]. The maps in panel D are traced from an image from the CIA World Factbook [https://www.cia.gov/library/publications/the-world-factbook/geos/ci.html]. The inset in panel B is courtesy of Alejandro López-Cortéz.)

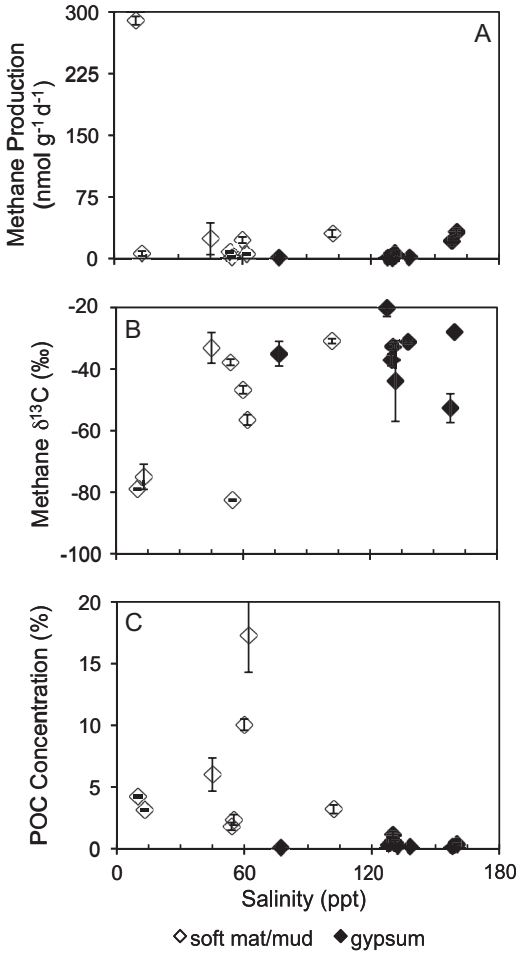

FIG 2 Methane production rates (A), methane $\delta^{13}C$ values (B), and POC concentrations (C) as a function of salinity.

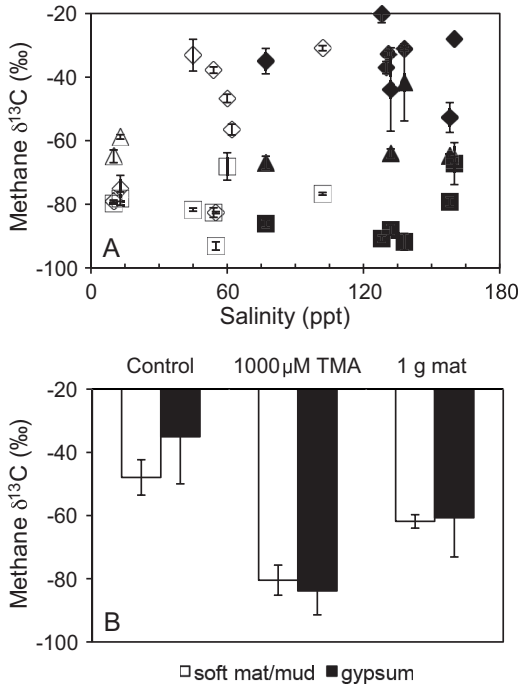

FIG 3 The $\delta^{13}C$ values of methane produced in unamended controls (diamonds), 1,000 μM TMA-amended (squares), and 1 g mat-amended (triangles) incubation vials as a function of salinity (A) and averaged overall (B). Soft-mat/mud (open symbols) and gypsum-hosted endoevaporite (closed symbols) sites are also differentiated.

amended vials ranged from 0.7 to 1910 nmol g^{-1} day^{-1} (Table 1). The methane $\delta^{13}C$ values produced from mat-amended vials ranged from −67 to −42‰ and were generally ^{13}C depleted relative to the unamended controls, although the mat-amended $\delta^{13}C$ values were not as ^{13}C depleted as the TMA-amended values (Table 1, Fig. 3). Similar to the TMA-amended vials, the $\delta^{13}C$ values from mat-amended, lower-salinity, soft-mat/mud sites were not different from the higher-salinity, gypsum-hosted sites (Student *t* test, $P > 0.8$).

DISCUSSION

The main purpose of the present study was to further investigate the biogenic production of methane with anomalously high, ^{13}C-enriched $\delta^{13}C$ values by microbial communities living within evaporitic minerals in hypersaline systems. The hypothesis of substrate limitation in these environments was tested by increasing the availability of TMA and organic matter to methanogens and observing any changes in the stable isotopic composition of the methane produced.

Similar to what Tazaz et al. (1) observed, the isotopic composition of methane produced by gypsum-hosted endoevaporite mats at the higher salinity sites was distinctly different from that produced by soft microbial mats/mud at the lower-salinity sites. The gypsum-hosted endoevaporite mats produced methane that was significantly enriched in ^{13}C, with $\delta^{13}C$ values ranging from −20 to −53‰. The endoevaporite mats also had significantly lower POC content than the soft microbial mats. It was this relationship between POC and methane $\delta^{13}C$ values that first suggested that substrate limitation plays a role in the isotopic composition of the methane (9).

Because the isotopic composition of the methane depends upon the isotopic composition of the substrate from which it is derived, fractionation factors are used to take the source material into account. However, since methane produced from environmental samples is generally derived from more than one substrate, apparent fractionation factors (28, 29) are usually determined. If the POC $\delta^{13}C$ value is used as a proxy for all substrates (see, for example, references 9 and 30), then the apparent fractionation factor (α) is calculated as follows: $\alpha = (\delta^{13}C\text{-POC} + 1{,}000)/(\delta^{13}C\text{-}CH_4 + 1{,}000)$, where $\delta^{13}C$-POC and $\delta^{13}C$-CH_4 are the stable isotopic compositions of POC and methane, respectively. In Fig. 4 it can be seen that the apparent fractionation factors are significantly higher, indicating more fractionation, for the soft microbial mat/mud sites than the gypsum-hosted endoevaporite mat sites. This suggests that substrate limitation, which decreases isotopic fractionation, may be occurring to a greater extent at the higher-salinity gypsum-hosted sites than at the soft-mat/mud sites.

Adding high concentrations of TMA increased the methane production rates, as expected (Table 1). In addition, the $\delta^{13}C$ values of the methane produced in the TMA-amended vials were significantly ^{13}C depleted (paired Student *t* test, $P < 0.01$) relative to those produced in the unamended controls (Fig. 3). The TMA-

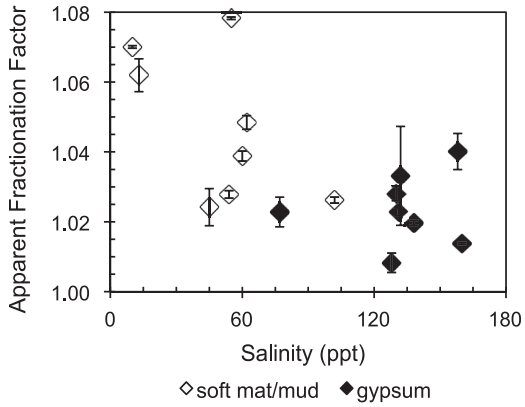

FIG 4 Apparent fractionation factors for methanogenesis in unamended control vials as a function of salinity.

amended vials had methane $\delta^{13}C$ values ranging from −93 to −67‰, easily falling within Whiticar's (13) biogenic range. All hypersaline sites, both soft-mat/mud and gypsum-hosted sites, exhibited a shift to lower, more ^{13}C-depleted methane $\delta^{13}C$ values with the addition of the TMA. On average, the soft-mat/mud sites shifted to lower values by about 30‰, whereas the average shift for the gypsum-hosted sites was about 50‰ (Fig. 3). This shift to lower, more commonly observed biogenic $\delta^{13}C$ methane values occurred at all hypersaline sites (both soft and endoevaporite mat sites), suggesting that substrate limitation may be a widespread phenomenon in hypersaline environments. The only site that did not show a significant decrease in the isotopic composition of methane with added TMA was ET2, the low-salinity mud site from the El Tatio geothermal field. For both years sampled, the unamended controls and the TMA-amended vials produced methane with $\delta^{13}C$ values in the low −70s‰ (Table 1). These similar and very ^{13}C-depleted $\delta^{13}C$ values suggest that the methanogens at this site were fully fractionating and not experiencing substrate limitation *in situ*.

It was curious that when dried, autoclaved microbial mat was added as a source of additional organic matter, methane production rates were not stimulated consistently across all sites. Instead, methane production rates increased (or stayed the same) at the Atacama sites, and decreased at Area 9, the only site tested at Guerrero Negro (Table 1). This decrease in methane production was unexpected, as the mat additions increased the organic carbon content in the incubations vials of Area 9 by 5- to 6-fold the original POC concentration (up to 1 to 2% POC in the samples). As noted above, organic carbon content in all vials was increased by 1.3- to 7-fold.

The mechanism by which the microbial mat amendments affected methane production rates and why rates were stimulated at the Atacama sites and inhibited at Area 9 in Guerrero Negro are unclear. One possible explanation is that with the increase in organic carbon content, caused by the addition of microbial mat, fermentation increased. Fermentation produces low-molecular-weight organic molecules, as well as H_2 and CO_2 (31). Increasing the H_2 concentration could let methanogens effectively compete with sulfate reducers for H_2, allowing methanogenesis by CO_2 reduction to occur. Increased fermentation and organic matter remineralization in the mat-amended vials is supported by higher headspace CO_2 concentrations in the mat-amended vials relative to unamended control vials (32). Although this explanation is consistent with increased methane production rates at the Atacama sites, it does not explain the inhibition observed at Area 9, since the methanogens at Area 9 should still produce methane at unamended control rates by using the substrates already present. However, if increased fermentation and growth of fermenters occurred, then competition for the osmolyte glycine betaine may have also occurred. Because of the energetic expense of biosynthesis, most halophilic or halotolerant heterotrophic microorganisms accumulate glycine betaine from the environment rather than synthesize it themselves (3, 33). If competition for any glycine betaine in the medium occurred, then this may have lessened the amount of TMA (derived from glycine betaine) in the environment, reducing the amount of methane produced from TMA and allowing for the grow-in of CO_2 reducing methanogens. Hydrogenotrophic (CO_2 reducing) methanogens are either not active or active to a small extent in the Guerrero Negro ponds and yet will increase in number when conditions become favorable (34, 35). At the Atacama sites, preliminary data from both Salar de Llamara and El Tatio suggest that the most abundant methanogens are members of the orders *Methanomicrobiales* and *Methanobacteriales* (B. Valenzuela et al., unpublished data). All members of both orders can use CO_2/H_2 (36); so if H_2 concentrations had in fact increased, methanogenesis could have immediately increased. Unfortunately, it is unknown whether H_2 concentrations were higher in mat-amended vials, since H_2 concentrations were not measured.

Similar to the TMA-amended vials, the methane $\delta^{13}C$ values of the mat-amended vials at the gypsum-hosted hypersaline sites, including Area 9, were also ^{13}C depleted, with values ranging from −67 to −42‰ (Table 1). The methane $\delta^{13}C$ values produced in mat-amended vials at site ET2, the only soft-mat/mud site tested, were higher than the unamended controls, rising from approximately −77 to −62‰ (averaged between sampling events/years). This mat-amended $\delta^{13}C$ value for ET2 (−62‰) is similar to the average of the gypsum-hosted sites (−61‰) (Fig. 3), suggesting a similar methanogenic pathway in these vials, perhaps CO_2 reduction.

Apparent fractionation factors have been used to infer pathways of methanogenesis in natural environments (30), since methanogens will fractionate carbon isotopes to various degrees depending on the substrate used (13, 29). The substrates can be ordered based on the amount of fractionation that occurs. This ordering, from least to greatest fractionation (with fractionation factors indicated in parentheses), is as follows: acetate (1.01 to 1.03), dimethylsulfide (1.04 to 1.05), CO_2/H_2 (1.03 to 1.08), trimethylamine (1.05 to 1.07), and methanol (1.07 to 1.09) (29, 37–39). The process of CO_2 reduction has been the most widely studied methane production pathway, encompassing both culture and environmental studies (29), which may explain why the widest range of fractionation factors is reported for this process. Although there is full overlap between fractionation factors for CO_2/H_2 and TMA, TMA falls at the higher end of the range (29, 39).

Unfortunately, because substrate limitation reduces isotopic fractionation, we cannot infer *in situ* pathways of methanogenesis from the unamended control vials using the above literature fractionation factors, since those fractionation factors were generally determined under nonlimiting conditions. However, with the TMA and mat amendments, substrate limitation appears to be

alleviated based on the ^{13}C-depleted methane δ^{13}C values relative to the controls and the fact that, on average, <20% of the TMA was used in the TMA-amended vials (median value = 9%). However, two hypersaline sites used more than 35% of the TMA amendment (Area 9 [March 2012] and Area 1 [November 2012]), if all of the methane produced came from the added TMA. These two sites had TMA-amended methane δ^{13}C values closer to the added TMA isotopic value (−40‰) than the other sites (Table 1) and so may not have been fractionating to the full extent possible. However, these two sites were still almost 30‰ more ^{13}C depleted than the added TMA.

The methane δ^{13}C values for the TMA-amended vials (−93 to −67‰) were consistently more ^{13}C depleted than those for the mat-amended vials (−67 to −42‰) (Fig. 3), pointing toward differences in pathways for methane production in these two amendment treatments. Within these treatment vials, the methane carbon can be derived both from the POC *in situ* and from the amendment, whether TMA or mat material.

To determine apparent fractionation factors for the mat-amended vials, isotopic mass balance calculations can be used to calculate the isotopic composition of the total organic carbon (POC plus mat addition) within the vials. Because of the low %POC at the gypsum-hosted endoevaporite mat sites (Table 1), the calculated isotopic composition of total organic matter within these mat-amended vials was dominated by the mat (−11‰), with δ^{13}C values ranging from −11.6 to −11.2‰. At the ET2 site, with its higher %POC (Table 1), the calculated isotopic compositions of total organic matter within the mat-amended vials were −16.0‰ in May 2012 and −13. 8‰ in May 2013. The apparent fractionation factors determined using these δ^{13}C values of the total organic carbon within the mat-amended vials, along with the δ^{13}C values of the resultant methane, range from 1.03 to 1.06. These factors are in the range of those determined for CO_2 reduction (29), supporting the hypothesis of increased fermentation and H_2 production leading to CO_2/H_2 methanogenesis with mat addition.

It would also be satisfying to calculate apparent fractionation factors for the TMA-amended vials to show that they fall within the range for TMA use from the literature. Although it is apparent that TMA is used for methanogenesis in the TMA-amended vials, determining apparent fractionation factors in this case is not easily accomplished. This is due to the large difference in δ^{13}C values between the TMA added (−40‰) and the POC *in situ* (−18 to −6‰) and to the fact that we do not know how much of either is used. If only added TMA was used to produce the methane, then the fractionation factors average 1.05 (range, 1.03 to 1.06). Presumably, some *in situ* TMA, as well as other substrates, was also used to some extent. If only POC-derived substrates were used (assuming these substrates, which would be part of the dissolved organic carbon pool, have similar isotope values as the POC [40]), apparent fractionation factors average 1.08 (range, 1.06 to 1.09). Simplistically, if half of the methane was produced by the added TMA and the other half derived from the POC, then apparent fractionation factors would average 1.06, a value that falls within the range for TMA use as determined by Summons et al. (38) and Londry et al. (39).

The data described here show that when either TMA or dried microbial mat (as a source of natural organic matter) was added to incubation vials, the isotopic composition of the methane produced had significantly lower ^{13}C-depleted δ^{13}C values at all hypersaline sites examined. This suggests that substrate limitation for methanogenesis may be a widespread phenomenon at these sites, with greater limitation (and so less fractionation) occurring at the gypsum-hosted endoevaporite sites than at soft-mat/mud sites. The δ^{13}C values of methane measured from TMA-amended vials were also significantly more ^{13}C depleted than methane from the mat-amended vials. This is consistent with greater fermentation in the mat-amended vials that could have allowed for a marked increase in methane production from CO_2/H_2 in these vials.

ACKNOWLEDGMENTS

This study was supported by NASA exobiology grants to C.A.K. and B.M.B.

We thank Exportadora de Sal, S.A., for access to field sites in Guerrero Negro, Mexico. We also thank Alfonso Davila, Jonathan García, José García Maldonado, and Bernardita Velenzuela for logistical and field help.

REFERENCES

1. **Tazaz AM, Bebout BM, Kelley CA, Poole J, Chanton JP.** 2013. Redefining the isotopic boundaries of biogenic methane: methane from endoevaporites. Icarus **224:**268–275. http://dx.doi.org/10.1016/j.icarus.2012.06.008.
2. **Oren A.** 2011. Thermodynamic limits to microbial life at high salt concentrations. Environ. Microbiol. **13:**1908–1923. http://dx.doi.org/10.1111/j.1462-2920.2010.02365.x.
3. **Oren A, Elevi Bardavid R, Kandel N, Aizenshtat Z, Jehlička J.** 2013. Glycine betaine is the main organic osmotic solute in a stratified microbial community in a hypersaline evaporitic gypsum crust. Extremophiles **17:**445–451. http://dx.doi.org/10.1007/s00792-013-0522-z.
4. **Reed RH, Chudek JA, Foster R, Stewart WDP.** 1984. Osmotic adjustment in cyanobacteria from hypersaline environments. Arch. Microbiol. **138:**333–337. http://dx.doi.org/10.1007/BF00410900.
5. **Oren A.** 1990. Formation and breakdown of glycine betaine and trimethylamine in hypersaline environments. Antonie Van Leeuwenhoek **58:**291–298. http://dx.doi.org/10.1007/BF00399342.
6. **Reeburgh WS.** 2007. Oceanic methane biogeochemistry. Chem. Rev. **107:**486–513. http://dx.doi.org/10.1021/cr050362v.
7. **Oremland RS, Polcin S.** 1982. Methanogenesis and sulfate reduction: competitive and noncompetitive substrates in estuarine sediments. Appl. Environ. Microbiol. **44:**1270–1276.
8. **King GM.** 1988. Methanogenesis from methylated amines in a hypersaline algal mat. Appl. Environ. Microbiol. **54:**130–136.
9. **Kelley CA, Poole JA, Tazaz AM, Chanton JP, Bebout BM.** 2012. Substrate limitation for methanogenesis in hypersaline environments. Astrobiology **12:**89–97. http://dx.doi.org/10.1089/ast.2011.0703.
10. **Schink B, Zeikus JG.** 1982. Microbial ecology of pectin decomposition in anoxic lake sediments. J. Gen. Microbiol. **128:**393–404.
11. **Mincer TJ, Aicher AC.** 2013. Production of methanol by a wide phylogenetic array of phytoplankton and implications for epibiont interactions, abstr. 12040. Abstr. ASLO 2013 Aquat. Sci. Meet. Association for the Sciences of Limnology and Oceanography, Waco, TX.
12. **Capone DG, Kiene RP.** 1988. Comparison of microbial dynamics in marine and freshwater sediments: contrasts in anaerobic carbon catabolism. Limnol. Oceanogr. **33:**725–749. http://dx.doi.org/10.4319/lo.1988.33.4_part_2.0725.
13. **Whiticar MJ.** 1999. Carbon and hydrogen isotope systematics of bacterial formation and oxidation of methane. Chem. Geol. **161:**291–314. http://dx.doi.org/10.1016/S0009-2541(99)00092-3.
14. **Coleman DD, Risatti JB, Schoell M.** 1981. Fractionation of carbon and hydrogen isotopes by methane-oxidizing bacteria. Geochim. Cosmochim. Acta **45:**1033–1037. http://dx.doi.org/10.1016/0016-7037(81)90129-0.
15. **Bebout BM, Hoehler TM, Thamdrup B, Albert D, Carpenter SP, Hogan M, Turk K, Des Marais DJ.** 2004. Methane production by microbial mats under low sulfate concentrations. Geobiology **2:**87–96. http://dx.doi.org/10.1111/j.1472-4677.2004.00024.x.
16. **Kelley CA, Prufert-Bebout LE, Bebout BM.** 2006. Changes in carbon cycling ascertained by stable isotopic analyses in a hypersaline micro-

bial mat. J. Geophys. Res. **111:**GO4012, http://dx.doi.org/10.1029/2006JG000212.
17. **Orphan VJ, Jahnke LL, Embaye T, Turk KA, Pernthaler A, Summons RE, Des Marais DJ.** 2008. Characterization and spatial distribution of methanogens and methanogenic biosignatures in hypersaline microbial mats of Baja California. Geobiology **6:**376–393. http://dx.doi.org/10.1111/j.1472-4669.2008.00166.x.
18. **McKay CP, Friedmann EI, Gómez-Silva B, Cáceres-Villanueva L, Andersen D, Landheim R.** 2003. Temperature and moisture conditions for life in the extreme arid regions of the Atacama Desert: four years of observations including the El Niño of 1997-1998. Astrobiology **3:**393–406. http://dx.doi.org/10.1089/153110703769016460.
19. **Javor BJ, Castenholz RW.** 1980. Laminated microbial mats, Laguna Guerrero Negro, Mexico. Geomicrobiol. J. **2:**237–273.
20. **Des Marais DJ, Cohen Y, Nguyen H, Cheatham M, Cheatham T, Munoz E.** 1989. Carbon isotopic trends in the hypersaline ponds and microbial mats at Guerrero Negro, Baja California Sur, Mexico: implications for precambrian stromatolites, p 191–203. *In* Cohen Y, Rosenberg E (ed), Microbial mats: physiological ecology of benthic microbial communities. ASM Press, Washington, DC.
21. **Canfield DE, Des Marais DJ.** 1993. Biogeochemical cycles of carbon, sulfur, and free oxygen in a microbial mat. Geochim. Cosmochim. Acta **57:**3971–3984. http://dx.doi.org/10.1016/0016-7037(93)90347-Y.
22. **Des Marais DJ.** 1995. The biogeochemistry of hypersaline microbial mats. Adv. Microb. Ecol. **14:**251–274. http://dx.doi.org/10.1007/978-1-4684-7724-5_6.
23. **Bebout BM, Carpenter SP, Des Marais DJ, Discipulo M, Embaye T, Garcia-Pichel F, Hoehler TM, Hogan M, Jahnke LL, Keller RM, Miller SR, Profert-Bebout LE, Raleigh C, Rothrock M, Turk K.** 2002. Long-term manipulations of intact microbial mat communities in a greenhouse collaborator: simulating Earth's present and past field environments. Astrobiology **2:**383–402. http://dx.doi.org/10.1089/153110702762470491.
24. **Ley RE, Harris JK, Wilcox J, Spear JR, Miller SR, Bebout BM, Maresca JA, Bryant DA, Sogin ML, Pace NR.** 2006. Unexpected diversity and complexity of the Guerrero Negro hypersaline microbial mat. Appl. Environ. Microbiol. **72:**3685–3695. http://dx.doi.org/10.1128/AEM.72.5.3685-3695.2006.
25. **Huerta-Diaz MA, Delgadillo-Hinojosa F, Siqueiros-Valencia A, Valdivieso-Ojeda J, Reimer JJ, Segovia-Zavala JA.** 2012. Millimeter-scale resolution of trace metal distributions in microbial mats from a hypersaline environment in Baja California, Mexico. Geobiology **10:**531–547. http://dx.doi.org/10.1111/gbi.12008.
26. **Rice AL, Gotoh AA, Ajie HO, Tyler SC.** 2001. High precision continuous-flow measurement of $\delta^{13}C$ and δD of atmospheric CH_4. Anal. Chem. **73:**4104–4110. http://dx.doi.org/10.1021/ac0155106.
27. **Hedges JI, Stern JH.** 1983. Carbon and nitrogen determinations of carbonate-containing soils. Limnol. Oceanogr. **29:**657–663.
28. **Chanton J, Chaser L, Glaser P, Siegel D.** 2005. Carbon and hydrogen isotopic effects in microbial methane from terrestrial environments, p 85–105. *In* Flanangan LB, Ehleringer JR, Pataki DE (ed), Stable isotopes and biosphere-atmosphere interactions: physiological ecology series. Elsevier Academic Press, London, United Kingdom.
29. **Conrad R.** 2005. Quantification of methanogenic pathways using stable carbon isotopic signatures: a review and a proposal. Org. Geochem. **36:**739–752. http://dx.doi.org/10.1016/j.orggeochem.2004.09.006.
30. **Potter EG, Bebout BM, Kelley CA.** 2009. Isotopic composition of methane and inferred methanogenic substrates along a salinity gradient in a hypersaline microbial mat system. Astrobiology **9:**383–390. http://dx.doi.org/10.1089/ast.2008.0260.
31. **Wüst PK, Horn MA, Drake HL.** 2009. Trophic links between fermenters and methanogens in a moderately acidic fen soil. Environ. Microbiol. **11:**1395–1409. http://dx.doi.org/10.1111/j.1462-2920.2009.01867.x.
32. **Nicholson BE.** 2013. Effect of increasing trimethylamine and organic matter concentration on stable carbon isotopes of methane produced in hypersaline, substrate limited environments. M.S. thesis. University of Missouri, Columbia, MO.
33. **Oren A.** 2001. The bioenergetics basis for the decrease in metabolic diversity at increasing salt concentrations: implications for the functioning of salt lake ecosystems. Hydrobiologia **466:**61–72. http://dx.doi.org/10.1023/A:1014557116838.
34. **García-Maldonado JQ, Bebout BM, Everroad RC, López-Cortéz A.** 10 August 2014. Evidence of novel phylogenetic lineages of methanogenic *Archaea* from hypersaline microbial mats. Microb. Ecol. http://dx.doi.org/10.1007/s00248-014-0473-7.
35. **Smith JM, Green SJ, Kelley CA, Prufert-Bebout L, Bebout BM.** 2008. Shifts in methanogen community structure and function associated with long-term manipulation of sulfate and salinity in a hypersaline microbial mat. Environ. Microbiol. **10:**386–394. http://dx.doi.org/10.1111/j.1462-2920.2007.01459.x.
36. **Garcia J-L, Patel BKC, Ollivier B.** 2000. Taxonomic, phylogenetic, and ecological diversity of methanogenic *Archaea*. Anaerobe **6:**205–226. http://dx.doi.org/10.1006/anae.2000.0345.
37. **Krzycki JA, Kenealy WR, DeNiro MJ, Zeikus JG.** 1987. Stable carbon isotope fractionation by *Methanosarcina barkeri* during methanogenesis from acetate, methanol, or carbon dioxide-hydrogen. Appl. Environ. Microbiol. **53:**2597–2599.
38. **Summons RE, Franzmann PD, Nichols PD.** 1998. Carbon isotopic fractionation associated with methylotrophic methanogenesis. Org. Geochem. **28:**465–475. http://dx.doi.org/10.1016/S0146-6380(98)00011-4.
39. **Londry KL, Dawson KG, Grover HD, Summons RE, Bradley AS.** 2008. Stable carbon isotope fractionation between substrates and products of *Methanosarcina barkeri*. Org. Geochem. **39:**608–621. http://dx.doi.org/10.1016/j.orggeochem.2008.03.002.
40. **Bauer JE, Haddad RI, Des Marais DJ.** 1991. Method for determining stable isotope ratios of dissolved organic carbon in interstitial and other natural marine waters. Mar. Chem. **33:**335–351. http://dx.doi.org/10.1016/0304-4203(91)90076-9.